ID: 637

Polystyrene-Induced Renal Oxidative Damage and Inflammation Mediated by PPARγ, IL-17, and MAPK8IP3 in Mice

Abdallah A. Basher[1,2], Saber Y. Adam[1], Chenhui Li[1], Abdelkareem A. Ahmed[3], Hao-Yu Liu[1,2], Widad A. Abdalla[1,2], Kennedy J. Ogamune[1,2], Hira Sayed[1], and Demin Cai[1,*]

[1] College of Animal Science and Technology, Jiangsu Key Laboratory of Animal Genetic Breeding and Molecular Design, Yangzhou University, Yangzhou 225009, PR China
[2] Joint International Research Laboratory of Agricultural & Agri-Product Safety, The Ministry of Education of China, Yangzhou University, Yangzhou 225009, China
[3] Department of Veterinary Biomedical Sciences, Botswana University of Agriculture and Natural Resources, Gaborone P.O. Box 100, Botswana

Abstract

Polystyrene-microplastics (PS-MPs) are pervasive environmental contaminants found in common household items, and their ingestion with dietary intake and water is linked to adverse health effects. Following ingestion, PS-MPs can translocate into the circulatory system and accumulate in tissues including kidney. Twelve 6-week-old male C57BL/6 mice were divided into a control group (n = 6) and a PS-MPs group (n = 6) administered 1 mg/kg/day of PS-MPs via oral gavage. Kidney tissue was subjected to histological analysis and thorough transcriptome profiling to identify dysregulated pathways. Histological examination revealed renal atrophy, hemorrhage, thinning of Bowmen's capsules, and increased Bowmen's capsules space in the PS-MPs group. TEM confirmed severe ultrastructural damage, including nuclear deformation, cytoplasmic vacuolization, and mitochondrial cristae disruption. Transcriptome analysis showed significant enrichment in the PPAR, MAPK, and inflammatory response signaling pathways. Key dysregulated genes included PPARG, ACADL, and SCP2 (PPAR pathway); *MAPK8IP3*, *MAPK11*, and *FGFR1* (MAPK pathway); and LI-17, *RELA*, and *TLR1* (inflammatory response). This study aimed to investigate the molecular mechanisms underlying PS-MPs-induced kidney injury in a mouse model, with a focus on transcriptomic changes in inflammatory and oxidative stress pathways. In male C57BL/6 mice, PS-MPs exposure induces significant kidney damage at histological, ultrastructural, and molecular levels, dysregulating genes critical to oxidative stress, inflammation, and identifies PPARγ, IL-17 and *MAPK8IP3* as pivotal mediators in PS-MPs-induced nephrotoxicity.

Key Words: *Polystyrene-microplastics; PPARγ; IL-17; MAPK8IP3; nephrotoxicity*

Introduction

Plastics are integral to modern life due to their durability, low cost, and versatility. Global plastic production exceeds 350 million tonnes annually, and a substantial proportion persists as waste that gradually degrades into microplastics (MPs), particles ranging from 0.1 μm to 5 mm [1-4]. Under environmental conditions, larger plastic materials fragment through physical abrasion, ultraviolet (UV) radiation, and photo-oxidative and thermal oxidation processes, along with biodegradation [5-7]. These processes contribute to the widespread distribution of microplastics in the environment.

Polystyrene microplastics (PS-MPs) can be transported over long distance through atmospheric dust, snow, wind, and atmospheric deposition, as well as through aquatic systems such as lakes, rivers, and oceans [8-10]. Consequently, PS-MPs have been detected in diverse environments, including urban area, forests, and remote locations such as the Swiss Alps and the glaciers of the Tibetan Plateau [11, 12]. In addition, washing synthetic textiles is well-recognized sources of microplastics (MPs) and nano plastic release into the environment [13].

Humans are exposed to MPs primarily through inhalation of airborne particles, ingestion of contaminated food and water, and dermal contact [14]. After ingestion, MPs may translocate into the circulatory system [15], and accumulate in tissues. Sub accumulation has been demonstrated in several animals models, including mouse organs and the muscle tissue of northern fulmars, suggesting the potential for in humans [16-18]. Dietary exposure to MPs has been reported in a variety of food products, including, fish [19], seafood [20, 21], sugar and honey [22], tea prepared using plastic teabags [23], beer [24], milk [25], tap water and sea salt [24], bottled water [26], and unfiltered water [27]. Previous studies estimate that humans may ingest approximately 0.1-5 g of microplastics (MPs) weekly, with an average blood concentration of about 1.6 μg/mL of plastic particles [28]. The continuous release of plastics into the environment and their persistence ecosystem have therefore raised significant public health concerns [29, 30].

Most studies investigating the nephrotoxic effects of microplastics (MPs) and nano plastics (NPs) have been published in the recent years. Li et al. demonstrated that polystyrene nanoplastics (PS-NPs) exacerbate lipopolysaccharide-induced apoptosis in mouse kidney cells through the oxidative stress endoplasmic reticulum pathways [31]. Another study shows that human renal cortical epithelial cells internalized PS-NPs (44 nm) via both endocytosis and passive diffusion [32]. Microplastic accumulation has been reported in aquatic organisms; for example, microplastics impair growth in crabs and accumulate in the kidneys of mackerel and scallops [33-35]. Furthermore, Tang et al. reported PS-MP-induced nephrotoxicity in mice associated with inflammation, oxidative stress and lipid disruption [36]. After six weeks of PS-NP exposure, mice exhibited renal tubular shrinkage, glomerular collapse, inflammatory cell infiltration, and impaired kidney function.

Accumulation of MPs in mouse kidneys has also been confirmed, with uptake observed in and HK-2 cells [32]. Exposure to PS-MPs increase mitochondrial reactive oxygen species (ROS) production, endoplasmic reticulum stress-related proteins, and inflammatory responses. In addition, PS-MP exposure elevates autophagy markers and inflammatory mediators. Enzymatic antioxidant responses are also altered, with increased superoxide dismutase (SOD) and glutathione peroxidase (GSH-Px) activity and significant inhibition of catalase (CAT). Pro-inflammatory cytokines, including TNF-α, IL-6, IL-10, and MCP-1, are significantly elevated. These changes are associated with weight loss, increased mortality, and histopathologically confirmed kidney injury in exposed mice. Similarly, Meng et al. reported that PS-MP exposure induces inflammation in chickens through activation of the NF-B pathways and modulates necroptosis through RIP1/RP3/MLKL signaling pathways [37].

Peroxisome proliferator-activated receptors (PPARs) regulate gene transcription through ligand-dependent and ligand-independent or independent mechanisms. They play essential role in fatty acid oxidation, lipid transport, glucose metabolism, adipogenesis, cholesterol metabolism, apoptosis, and inflammatory responses [38]. The PPAR family consists of three isoforms-PPAR-α, PPAR-β/δ, and PPAR-γ which differ in ligand specificity, tissue distribution, and physiological function [39]. Numerous experimental and clinical studies have demonstrated that PPARs play crucial role in maintaining renal energy homeostasis and lipid metabolism [40].

Mitogen-activated protein kinases (MAPKs) are functionally related kinases that regulated Key cellular processes involved in kidney disease, including cell survival, death, differentiation, and proliferation [41]. MAPK signaling cascades ultimately regulate transcription and downstream kinases that control gene expression through transcriptional and post-transcriptional mechanisms [42]. Despite growing evidence of microplastic-induced nephrotoxicity, the molecular mechanisms by which polystyrene microplastics influence genes associated with PPARs and MAPK signaling pathways remain poorly understood.

Therefore, this study aimed to investigate the detrimental effects of polystyrene microplastics on inflammation, oxidative stress, and histopathological alterations in mouse kidneys, with particular focus on the modulation of the PPARg/RPS6KA5 and IL17 signaling pathways.

Material and methods

Animals

Twelve 6-week-old male C57BL/6 mice (weight 24 ± 2.1 g) were obtained from the Jiangsu Laboratory Animals Science Center (Jiangsu, China). For this initial mechanistic investigation, male mice were used to establish baseline effects of PS-MPs while avoiding potential confounding factors associated with female physiology and disease progression.

Animals were housed under controlled environmental conditions (22°C, 50% relative humidity, 12-hour light/12-hour dark cycle) with *ad libitum* access to a standard chow diet (Table 1) and drinking water. After a one-week acclimation period, the mice were randomly assigned to two groups (n=6/group): a control (Control) group, and the polystyrene microplastic (PS-MPs) treatment group.

The control group received phosphate-buffered saline (PBS), via daily oral gavage, The treatment group received PS-MPs. PS-MPs (1 μm particle size; Tianjin Baseline Chrom Tech Research Center, Beijing, China) suspended in PBS. Based on previous studies demonstrating renal accumulation of microplastics [36], and to simulate chronic, low-level human exposure [22, 37], mice in the treatment group were administered PS-MPs via oral gavage at a dose of 1 mg/kg/day for 28 consecutive days. The control group received an equivalent volume of PBS.

On day 29, all mice were euthanized at zeitgeber time (ZT) 8 (8 hours after lights on) [38], by intraperitoneal injection of pentobarbital sodium (80 mg/kg body weight; GENIA Biotech, Beijing, China). The kidneys were immediately excised, snap-frozen in liquid nitrogen, and stored at -80°C until further analysis.

Kidney H&E and immunohistochemical staining

The kidney tissue was stained with hematoxylin and eosin. Sections of kidney were preserved in a 4% paraformaldehyde solution. Sections were initially subjected for 10 and 5 minutes, respectively, to xylene and ethanol solutions. They then underwent a 5-minute hematoxylin staining, a 5-minute water wash, and a 1 to 3-

minute eosin solution staining. We then sealed it after being cleaned with ethanol. Lastly, the morphology was examined under a microscope. Kidney sections were incubated separately for 12 hours at 4°C with a primary antibody that targets KIM-1, HO-1, and IL-17, respectively, at a dilution of 1:200 for immunohistochemistry staining. The sections were then treated at 26°C with a diluted 1:100 goat anti-mouse/rabbit conjugated secondary antibody. All images were taken with Nikon Corporation fluorescence microscope, and ImageJ software was used to examine the staining region. All histopathological sections were evaluated by two independent investigators who were blinded to the group assignments (Control. vs PS-MPs) during the analysis and image acquisition.

Table 1. Product composition analysis guaranteed value for the basal diet (content per kg)

Items	***Per kg***
Moister	100g
Grude protein	200g
Grude fat	40g
Coarse fiber	50g
Coarse ash content	80 g
Calcium	10.18 g
Total phosphorus	12g
Lysine	13.2g
Methionine + cystine	7.8g
VA	14000 IU
Folic acid	6 mg
VE	120 IU
VD	1500 IU
Iron	120mg
Manganese	75 mg
Zinc	30 mg
Selenium	0.1- 0.2 mg

VA= vitamin A; VE = vitamin E; VD = vitamin D

Western blotting analysis

Kidney tissue was homogenized using the mixture after phosphatase and protease inhibitors were added to cell lysis solution (Biosharp, BL509A Hefei, China). Following the equilibration of their protein content, samples were separated on 10% SDS-PAGE gels. Samples were blocked for an hour with 5% skim milk against *KIM-1, HO-1, IL-171*, and *β-actin* (loading control) after being transferred to PVDF membranes (Millipore, IPVH00010, Burlington, CA, USA). Before being treated with HRP-conjugated secondary antibodies, membranes were first exposed to certain primary antibodies for duration of 12 hours at 4 °C. Finally, chemiluminescence was identified using a high-sensitivity ECL kit (NCM Biotech, P2300, Suzhou, China) and a Dannon 5200 multi-imaging system.

Transmission electron microscopy (TEM)

Small pieces of kidney tissues (~1.5 mm^3) from each group were fixed overnight at 4° C in 0.1 M a solution of 2.5% glutaraldehyde in phosphate buffer (pH7.4). The samples were then washed three times with phosphate-buffered saline (PBS) and post-fixed with 1% osmium tetroxide in the same buffer for 1-2 hours at room temperature. Following post-fixation, the tissues were washed three times in PBS, dehydrated through a graded ethanol series, and embedded in epoxy resin. Ultrathin sections (60-80 nm) were prepared using ultramicrotome, and stained with uranyl acetate and lead citrate. Images were captured using TEM (HT7800; Hitachi system, China). Ultrastructural evaluation was performed by an experienced pathologist blinded to the group assignments (Control. vs PS-MPs).

Quantitative real-time PCR

Mice kidney tissue was used to extract total RNA using the TRizol method as directed by the manufacturer (Thermo Fisher, Waltham, USA). Protein-nucleic acid assay (ND-2000UV, Thermo Fisher, Waltham, USA) and 1% agarose gel electrophoresis were used to determine the amount and quality of RNA. The All-in-One First-Strand cDNA Synthesis Super MIX for qPCR kit (QIAGEN, Frankfurt, Germany) was used to reverse-transcribe the RNA into cDNA. Nuclease-free H2O was added to 10 μL of the reverse transcription system, which included 0.5 μg of total RNA, 5 ×TransScript All-in-one SuperMix for qPCR, and 0.5 μL of gDNARemover. The reaction process is as follows: 15 minutes at 42 °C and 5 seconds at 85 °C. After reverse transcription, 90 μL of nuclease-free water is added and kept at -20 °C. 10 μL of PCR reaction mixture, comprising 1 μL of cDNA, 5 μL of 2 × Per-fectStart TM Green qPCR SuperMix, 0.2 μL of forward primer, 0.2 μL of reverse primer, and 3.6 μL of nuclease-free water, were used to perform real-time PCR using a LightCycler® 480 II Real-time PCR Instrument (Roche, Basel, Switzerland) with a PCR efficiency of 94 to 105%. In 384-well optical plates (Roche, Basel,

Switzerland), the reactions were incubated for 30 seconds at 94 °C. This was followed by 45 cycles of 5 seconds at 94 °C and 30 seconds at 60 °C. To confirm the precise generation of the anticipated PCR product, the melting curve analysis was carried out at the conclusion of the PCR cycle. Every sample was subjected to three separate analyses. Using the AceQ® qPCR SYBR Green Master Mix (Vazyme, Nanjing, China), qRT-PCR analysis was carried out using an ABI StepOne Plus Real-Time PCR System (Applied Biosystems, CA, USA). The 2-ΔΔCt method was used to calculate the expression levels of mRNAs after normalising them to the glyceraldehyde-3-phosphate dehydrogenase (GAPDH).

RNA-Seq and GSEA Analysis

Total RNA was extracted from the kidney tissue of the PS-MPs group and the control group of mice using 1 milliliter of trizol (Invitrogen, Waltham, MA, USA). RNA quality was assessed using an Agilent Bioanalyzer 2100 system (Agilent Technologies, CA, USA) was used to assess the quality of the extracted RNA. At Kidio Biotech Ltd., high-throughput sequencing was carried out utilizing the Illumina sequencing platform. The mouse gene expression reference GRCm38 was used to align the raw data. Trim Galore v0.6.5 (Babraham Bioinformatics - Trim Galore!), STAR v2.7.10b (GitHub - alexdobin/STAR: RNA-seq aligner), and rsem v1.3.3.1 were used to handle the raw data. FPKM, or fragments per kilobase of the exon model per million mapped fragments, was finally selected for further data analysis.

Gene Set Enrichment Analysis (GSEA 4.1.0) software was used to identify GO terms enriched in differentially expressed genes (DEGs) [39, 40]. Furthermore, the Metascape database (http://metascape.org/) was used to rank and categorize pathways of statistically enhanced biological processes among DEGs, for GO and KEGG pathways [41]. The Venn diagram, KEGG pathway plot, and volcano plot were created using an online data analysis and visualization platform (http://www.bioinformatics.com.cn).

Statistical Analysis

All data were analyzed using GraphPad (Prism 9.0.). The normality of data distribution was first assessed using **D**'Agostino-Person omnibus normality test. For data passing normality, two-tailed Student's t tests were used. Data are displayed as Mean values ± SEM. A *P*-value <0.05 was statistically Significant.

Result

Kidney H&E and immunohistochemical staining and Western blotting result

In this study the Control group of mice had shown the normal histological structure of renal cortex enclosing renal corpuscle with intact Bowman's capsule and glomerulus (Black arrow), proximal (Green arrow) and distal (Green arrow) convoluted tubules. Treatment group (PS-MPs) shows a significant ($P < 0.05$) renal damage evidenced by atrophy of the renal corpuscle (Black arrows), hemorrhage (white arrows), as well as a few Bowmen's capsule noticed with a very thin thickness (red arrow), and others with increase in Bowmen's space and decrease of glomerulus size compared to Control group of mice, (Figure 1A). Immunohistochemistry results showed that, PS-MPs-treated mice have high expression of KIM-1, HO-1, and IL-17, respectively, compared to mice in control group, (Figure 1B). However, to further confirm the expression of *KIM-1, HO-1, and IL-17*, we conducted western blot analysis, and the result shows that the protein levels of *KIM-1, HO-1, and IL-17* were significantly increased in the PS-MPs-treated mice compared to the control group (Figure 4C).

Ultrastructural changes after PS-MPs exposure

Consistent with our predictions of PS-MPs-induced renal damage, we assessed ultrastructural injuries in mouse kidney tissue using transmission electron microcopy (TEM). The TEM analysis revealed significant pathological alterations in renal cells of PS-MPs-treated mice compared to control. As shown in (Figure 2, a1-a4), renal cells from control (Control) group exhibited normal ultrastructure, including intact nuclei with dark heterochromatin (n) and mitochondria (m) with typical morphology. In contrast, cells from PS-MPs-exposed mice displayed severe ultrastructural damage (Figure 2, b). Key observations included, nuclear abnormalities, the nuclei showed uniform depression, deformation of the nuclear membrane, and condensation of chromatin that was marginated at the nuclear periphery (white arrows, Figure 2, b1). Cytoplasmic alterations, cytoplasm contained numerous lipid droplets (LD) and exhibited extensive vacuolization (red arrows, Figure 2, b1-b3). Mitochondria damage, mitochondria exhibited a rounded morphology (Figure 2, b1), along with disrupted cristae, swelling, and rupture of the outer membrane (Figure 2, b4).

Analysis of pathway enrichment

Transcriptome analysis was performed out using kidney tissue from the PS-MPs-treated group and the Control group in order to identify transcriptional pathways dysregulated by PS-MPs. The overall effect of PS-MPs treatment on gene expression is visualized in the volcano plot. Which displays significantly up- and down-regulated genes between the two groups (Figure 3A).

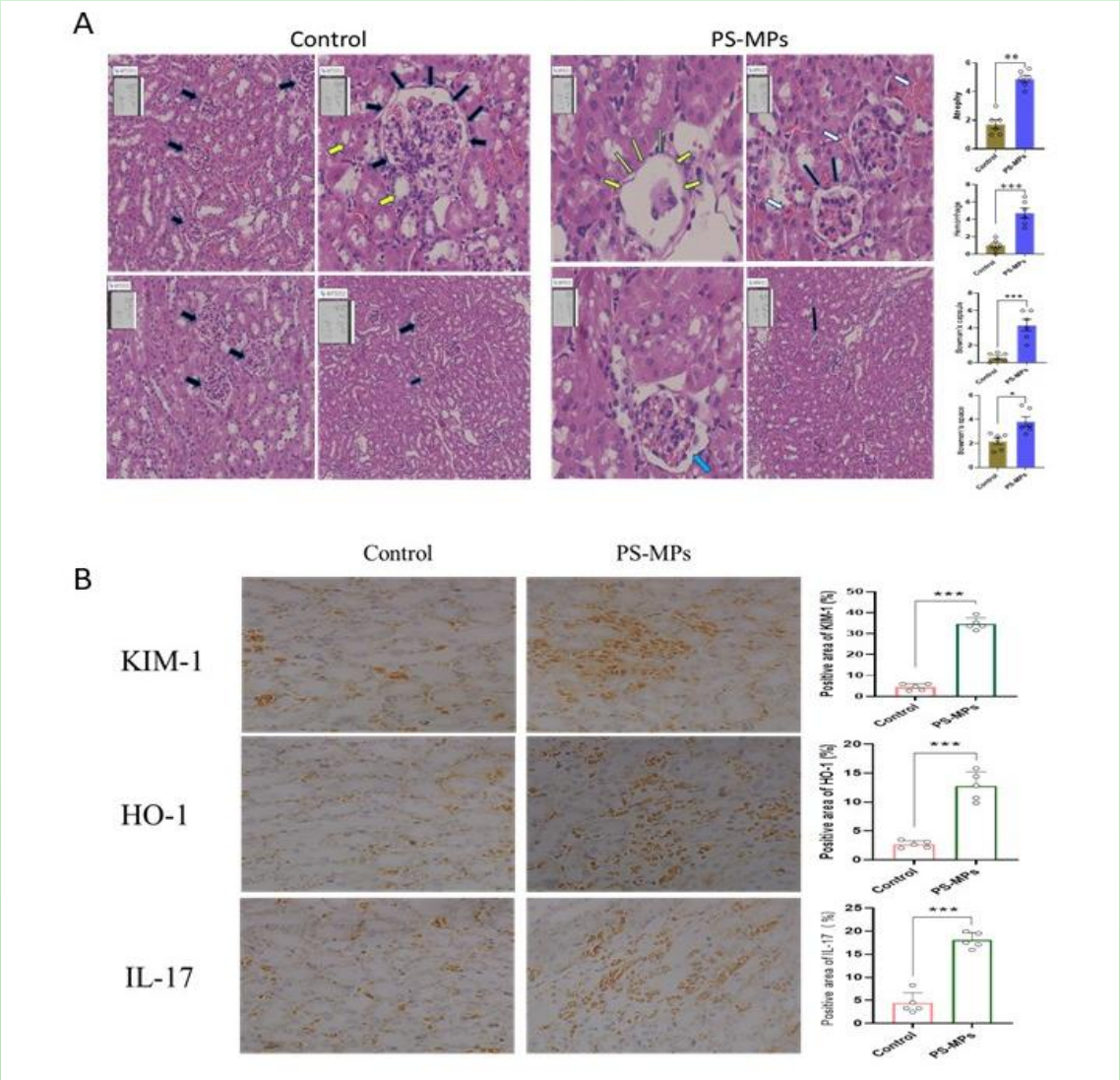

Figure 1. Histopathological and immunohistochemical assessment of kidney tissue following Polystyrene Microplastics (PS-MPs) exposure.

(A) Histopathological analysis: Control group; representative photomicrograph showing normal renal cortex histology with intact renal corpuscles, Bowman's capsule (black arrow), and convoluted tubules (yellow arrows). PS-MPs: Representative photomicrograph showing pathological damage including, renal corpuscle atrophy (black arrow), hemorrhage (white arrows), thinning of Bowmen's capsule (blue arrow), increased bowmen's space and decreased glomerulus size (yellow arrows). Quantitative analysis of renal corpuscle atrophy, hemorrhage, Bowman's capsule thickness, and Bowman's capsule space. Scale bar, 20, 50 µm. Data are presented as mean ± Standard Error of the Mean (SEM) (n=6). **(**B) Immunohistochemical analysis: Representative microscopic image of immunohistochemical staining and statistical assessment shown the protein expression of Kidney Injury Molecule-1 (KIM-1), Heme Oxygenase-1 (HO-1), and Interleukin-17 (IL-17) of kidney tissues in each group (Scale bars = 50 µm). (C) Western blot analysis *of KIM-1*, *HO-1*, and *IL-17* protein levels. * Indicates a significant difference from the Control group (*, $p < 0.05$; **, $p < 0.01$; ***, $p < 0.001$) as determined by Student's t-test

After calculating fold changes, low-count genes were filtered out using a standardized statistical threshold, and remaining database was analyzed using GSEA version 4.1.0. Genes from the Control versus PS-MPs comparison were highly enriched in cellular components including the cytoplasm, cytosol, enzyme binding, mitochondrial inner membrane, mitochondrion, and in the molecular function of enzyme binding (Figure 3B). Up-regulated differentially expressed genes (DEGs) were enriched in pathways Retinol metabolism, Cytokine-Cytokine receptor interaction, MAPK signaling, Linoleic metabolism, Calcium signaling, Metabolism of xenobiotic by cytochrome P450, PPAR signaling, Fatty acid degradation, and Fatty acid metabolism pathways, (Figure 3C). A cnetplot displays the specific genes linked to these pathways (Figure 3D). Down-regulated DEGs were enriched in KEGG, including Calcium signaling, Cytoskeleton in muscle cell, PPAR signaling, MAPK signaling, Pi3k-Akt signaling, Renin secretion, Inflammatory mediator regulation of TRP channels, Cytokine-cytokine receptor interaction, NOD-like receptor signaling, and Osteoclast differentiation pathways, (Figure 3E). A corresponding cnetplot for the down-regulated genes is shown in Figure 3F.

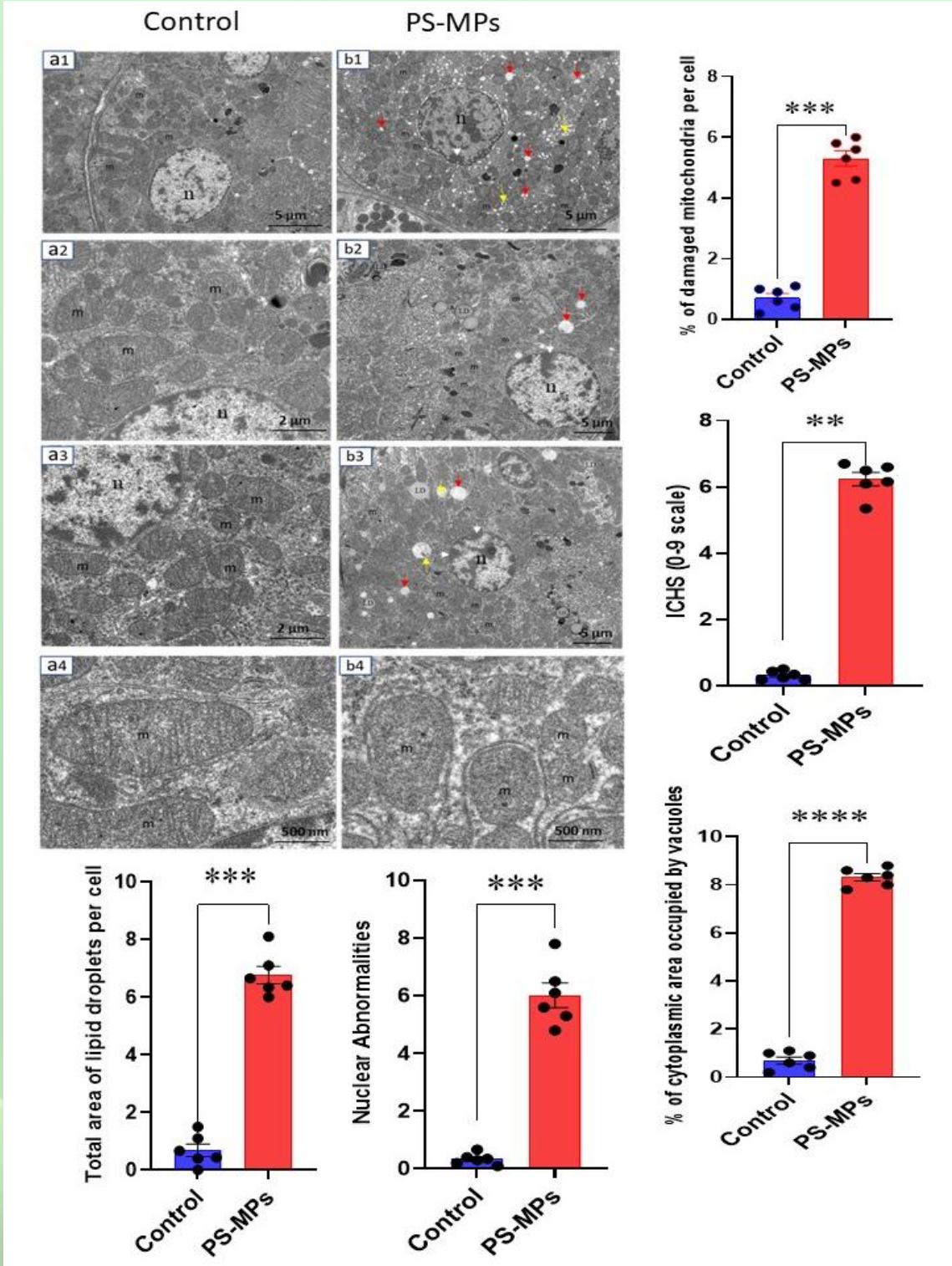

Figure 2. Ultrastructural analysis of renal cells following Polystyrene Microplastics (PS-MPs) exposure. Control group showing normal ultrastructure: a nucleus (n) with evenly distributed chromatin, an intact nuclear membrane (a1), and mitochondria (m) with typical morphology (a1-a4). PS-MPs group: displaying significant pathological alteration, nuclear abnormalities with condensed, marginated chromatin and irregular nuclear membrane (white arrows, b1); Cytoplasmic vacuolization (red arrows; b1-b3), and accumulation of lipid droplets (LD), a hallmark of inflammation, (yellow arrow; b1-b3). And severe mitochondrial damage (m) characterized by rounding, loss of cristae, outer membrane swelling and rupture (b1-b4). Scale bars, 2 µm, 5 µm, 500 µm. Quantitative analysis of damaged mitochondria per cell, integrated cellular health score (ICHS), cytoplasmic area occupied by vacuoles, nuclear abnormalities, total area of lipid droplets per cell * Indicates a significant difference from the Control group (*, $p < 0.05$; **, $p < 0.01$; ***, $p < 0.001$; ***, $p < 0.001$) as determined by Student's t-test.

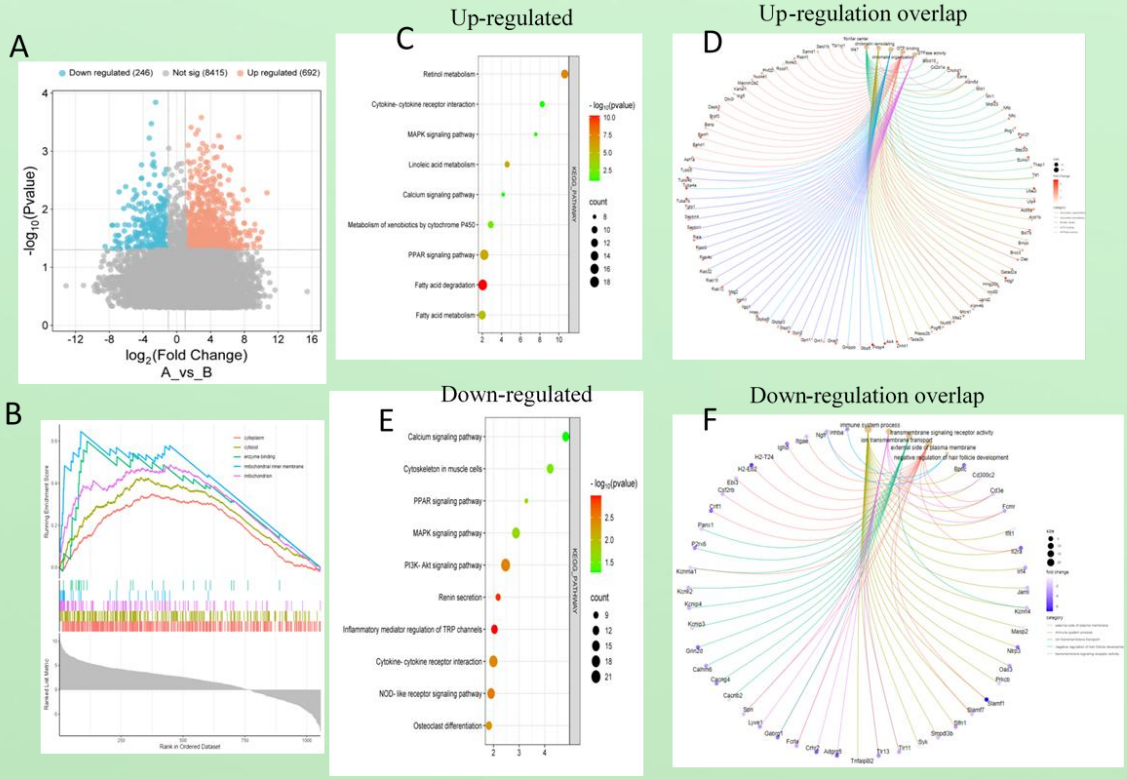

Figure 3. Transcriptomic profiling and pathway enrichment analysis of Differentially Expressed Genes (DEGs). (A) Volcano plot visualizing DEGs between the Control and Polystyrene Microplastics (PS-MPs) groups. The thresholds were set at |log2(fold change) | ≥ 2 and adjusted *p*-value < 0.05. Red points represent significantly up-regulated genes, blue points represent down-regulated genes, and gray points represent non-significant genes. (B) Gene Ontology (GO) enrichment analysis showing the top cellular components and molecular functions for the identified DEGs. (C) Kyoto Encyclopedia of Genes and Genomes (KEGG) pathway enrichment analysis for up-regulated DEGs. (D) Cnetplot displaying the relationships between the enriched KEGG pathways from (C) and the core genes within them. (E) KEGG pathway enrichment analysis for down-regulated DEGs. (F) Cnetplot displaying the relationships between the enriched KEGG pathways from (E) and the core genes within them.

DEGs interaction and gene expression analysis

The GO and KEGG pathway enrichment analysis of DEGs revealed that gene expression involved in PPAR signaling pathway and MAPK signaling pathway were among the most enriched pathways analyzed by gene ontology and KEGG, (Figure 4A). Therefore, we selected key differential genes of PPAR signaling pathway, MAPK signaling pathway, and Inflammatory response from biological process genes, and further analysis. STRING analysis predicted the relationship between these genes, showing they were highly correlated and interconnected (Figure 4B). We generated heatmaps displaying the expression profile for genes associated with PPAR signaling pathway (Figure 4C) MAPK signaling pathway (Figure 4D), and Inflammatory response signaling pathway (Figure 4E). These data suggest that PS-MPs might affect the mice kidney through modulation PPAR, MAPK, and Inflammatory response signaling pathways.

Quantitative real-time PCR gene expression

To further verify the expression pattern of DEGs for PPAR signaling pathway, MAPK signaling pathway, and inflammatory response from biological process, we measured the kidney-specific expression genes by qRT-PCR as displayed in (Figure 5). We found that the mRNA expression of ACADL, SCP2, EHHADH, CD36, HMGGS1, SLC27A2, PPARG, PCK1, SCD1, and ACAA1A involved in PPAR signaling pathway were significantly ($p < 0.05$) up-regulated in PS group compared to Control group, (Figure 5A). Moreover, the mRNA expression of MAPK8IP3, FGFR1, HSPB1, TAOK2, RRAS2, PAK2, MEF2C, CSF1, NGF, MAPK11, CACNA1C, HSPA1L, TGFB3, and RPS6KA5 involved in MAPK signaling pathway were significantly ($p < 0.05$) up-regulated in PS-MPs group compared to Control group, (Figure 5B). Finally, for inflammatory response, we selected overlapping genes in inflammatory response for up- and down-regulated DEGs for further qRT-PCR measurement. We found that the the mRNA expression of IL-17, RELA, SCYL3, MYD88, TLR12, ELF3, TNFRSF1B, CXCL9, TNFAIP3, and TLR1 were significantly ($p < 0.05$) up-regulated in PS-MPs group compared to Control group, (Figure 5C). These results show that PS-MPs administration in the dose at 1 mg/kg/day for 28 days can be remarkably cause oxidative stress and inflammation in the mice kidney via modulation of related genes involved in PPAR, MAPK, and inflammatory response signaling pathways.

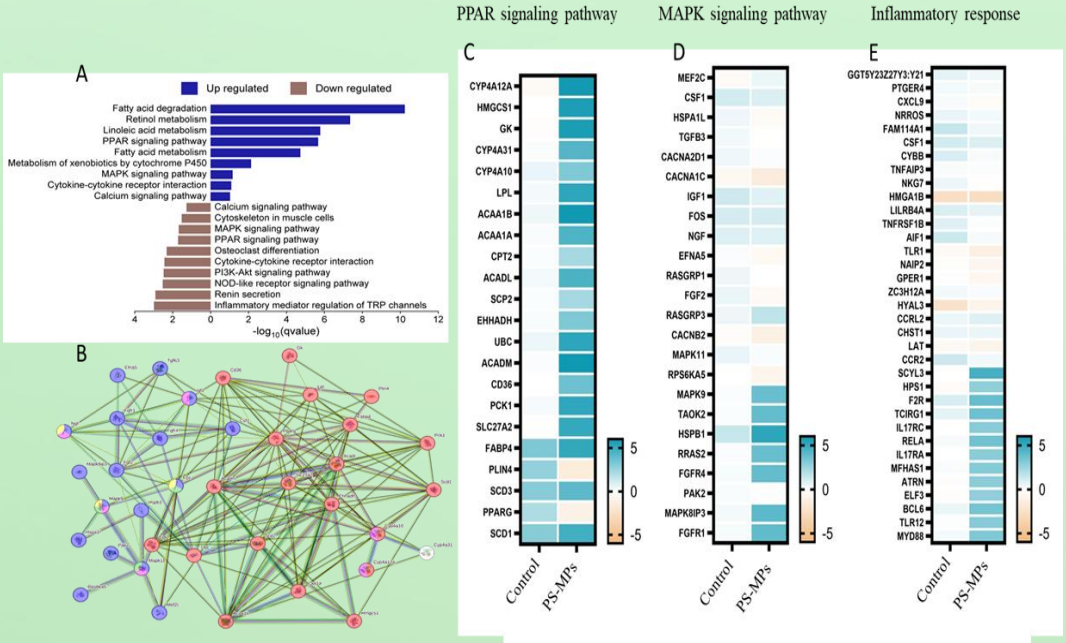

Figure 4. Interaction network and expression profiles of key signaling pathways.
(A) Gene Ontology (GO) analysis showing the normalized enrichment scores (NES) for significantly altered biological pathways between the Control and Polystyrene Microplastics (PS-MPs) groups. (B) Protein-protein interaction network generated using STRING database, showing the interactions between key genes from the Peroxisome Proliferator-Activated Protein Receptor (PPAR) signaling pathway, inflammatory response, Mitogen-Activated Protein Kinase (MAPK) signaling pathway, and Interleukin-17 (IL-17) signaling pathway. (C-E) Heatmaps displaying the expression profiles of significantly dysregulated genes associated with the (C) PPAR signaling pathway, (D) MAPK signaling pathway, and (E) inflammatory response, as annotated by the Kyoto Encyclopedia of Genes and Genomes (KEGG) database.

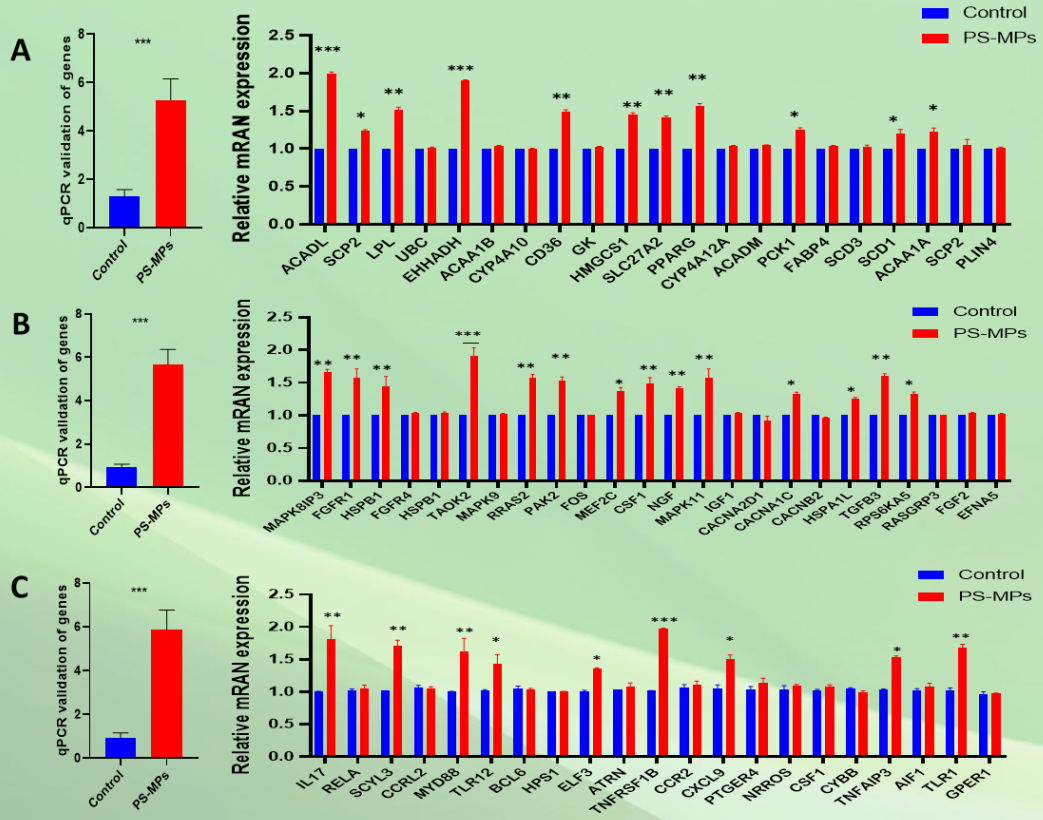

Figure 5. Quantitative Real-Time Polymerase Chain Reaction (qRT-PCR) validation of pathway-specific gene expression.
mRNA expression levels of key genes from the (A) the Peroxisome Proliferator-Activated Protein Receptor (PPAR) signaling pathway, (B) Mitogen-Activated Protein Kinase (MAPK) signaling pathway, and (C) inflammatory response were measured by qRT-PCR. Results are presented as relative expression (2^(-ΔΔCt)) compared to the Control group, which was set to 1. Data are presented as mean ± Standard Error of the Mean (SEM) (n=6). Asterisks indicate significant differences from the Control group as determined by Student's t-test (*, $p < 0.05$; **, $p < 0.01$; ***, $p < 0.001$).

Discussion

Microplastics have attracted increasing attention due to their widespread presence in the environment and their frequent detection in food and drinking water. These particles have been identified seafood, tap water, water bottles, sugar, salt, honey, and plastic-packaged foods. After ingestion, microplastics can enter internal organs including the kidney, where they may induce cellular damage [42]. Dietary intake therefore represents a major route human exposure, linking microplastics toxicity directly to food safety and nutritional health [43]. In the present study, we investigated the effect of polystyrene microplastics (PS-MPs) administrated at 1mg/kg/day for 28 days on mouse kidneys using transcriptome analysis. Our findings revealed substantial alterations in genes and signaling associated with immune response, inflammation, and oxidative stress.

The kidney represents a critical target organ in nanoplastics toxicity studies due to its essential role in the filtration and excretion of xenobiotics. Nanoplastics (NPs) originating from various physiological systems may accumulate in the kidney during clearance, potentially disrupting normal renal metabolism and glomerular filtration processes, thereby impairing kidney function. Ultrafine particulate matter to exert similar renal effects. For instance, a positive correlation has been observed between exposure to ultrafine particulate matter derived from motorcycle exhaust and kidney injury in mice [44]. Previous studies have reported that 5 μm MPs accumulate within the tubular epithelium of mouse kidneys [45]. Additionally, bioaccumulation of 50 nm polystyrene-nanoplastics (PS-NPs) and 0.3–4 μm polystyrene microplastics PS-MPs has been shown to induce histopathological damage in renal tissues [46]. Exposure to 1000 nm PS-MPs can lead to pathological changes in renal tissue, promote renal cell death, and alter serum biomarkers including urea nitrogen, creatinine, and inflammatory markers in rats [47]. Although several studies have demonstrated the accumulation of PS-MPs in mouse kidneys, the underlying regulatory mechanisms of renal injury remain insufficiently understood [20, 48]. In the present study, histological examination revealed renal corpuscle atrophy, hemorrhage, thinning of Bowmen's capsules in some regions, enlargement of Bowmen's space and reduction in glomerulus size in PS-MPs-treated mice compared to the Control group animals.

Kidney injury molecule- 1 (KIM-1) is a well-established biomarker of renal tubular injury. The elevated expression of KIM-1 observed in PS-MP-exposed mice suggests that exposure microplastics exposure induces renal tubule stress or damage. This observation aligns with broader evidence that environmental toxicants, such as heavy metals, can contribute to kidney disease [49, 50]. Heme oxygenase-1 (HO-1) is a stress-responsive enzyme that plays a key role in cellular defense against oxidative stress. The increased expression of MO-1 in PS-MPs-treated mice enhanced oxidative stress induced by microplastics exposure, thereby triggering an adaptive antioxidant response [51]. Activation of HO-1 is commonly observed under conditions of in inflammatory and oxidative stress and constitutes an essential component of cellular protective mechanisms [53]. HO-1 overexpression has been shown to reduce inflammation and neutralize toxic metabolites, thereby limiting cellular damage.

Interleukin- 17 (IL-17), a pro-inflammatory cytokine primarily produced by T helper 17 (Th17)cells, plays a crucial role in immune responses, particularly in host defense against pathogens [54]. Elevated IL-17 PS-MPs-treated mice suggest activation of the immune system and induction of an inflammatory response [55]. Microplastics may acts as foreign bodies within tissues, triggering immune response activation and promoting the release of pro-inflammatory cytokines such as IL-17 [56]. Increased IL- 17 expression following PS-MPs exposure may therefor reflect either a dysregulated inflammatory response contributing to tissue damage or host defense mechanism attempting to eliminate foreign particles. Consistent with these findings immunohistochemistry (IHC) and western blot analyses demonstrated significantly increased expression KIM-1, HO-1, and IL-17 in PS-MP-treated mice compared to control animals. Collectively, the simultaneous elevation of these biomarkers provides a comprehensive indication of PS-MP-induced nephrotoxicity. The observed systematic inflammatory response (IL- 17), oxidative stress and cellular defense activation (HO-1), and direct tubular injury (KIM-1) strongly suggest that PS-MP exposure imposes significant physiological stress on renal tissues. These findings highlight the potential ecological and health risks posed by microplastics, which can accumulate in ecosystems and enter biological systems through food chains [57]. Further studies are required to elucidate the long-term health consequences of microplastic exposure and to develop effective environmental mitigation strategies.

Consistent with the histological observations, our ultrastructural analysis further revealed profound subcellular damage in renal cells. Severe nuclear abnormalities, including membrane deformation and chromatin margination, were observed together with extensive cytoplasmic vacuolization, and mitochondrial damage characterized by swelling and membrane rupture. These morphological alterations represent hallmark features of cellular stress and apoptosis, strongly supporting our transcriptome findings indicating dysregulation of pathways associated with oxidative stress and inflammation. In particular, mitochondrial damage, in particular, provides a direct ultrastructural correlate for the oxidative stress processes identified in the transcriptional analysis. [58]

A notable finding of this study is the up-regulation of genes involved in the PPARs signaling pathway following PS-MPs exposure. PPARs are nuclear receptors that play a key role in regulating oxidative stress, inflammation,

and metabolic processes [59, 60]. Among the PPAR isoforms, PPARγ regulates genes associated with glucose and lipid metabolism, inflammatory responses, and cellular differentiation [62]. Three major subtypes have been identified: PPARα, PPARγ, and PPARβ/δ [63]. These isoforms exhibit distinct tissue distribution patterns that may contribute to their specific biological functions in different organs, including the kidney. PPARs target genes are primarily involved in adipogenesis, lipid metabolism, insulin sensitivity, glucose homeostasis, and cell growth and differentiation [64]. Consistent with these role, our transcriptomic data revealed that PS-MPs exposure significantly up-regulated multiple genes within the PPAR signaling pathway, including ACADL, SCP2, EHHADH, CD36, HMGGS1, SLC27A2, PPARG, PCK1, SCD1, and ACAA1A, which are associated with oxidative stress response, metabolism regulation, glucose homeostasis, inflammatory signaling.

In addition to PPAR signaling, our study identified significant up-regulation of genes involved in the mitogen-activated protein kinase (MAPK) signaling pathways. MAPK pathways play a central role in regulating cell growth, proliferation, survival, and stress responses [65, 66]. The canonical MAPK signaling cascade is typically initiated by the interaction of growth factors with their corresponding receptors often receptor tyrosine kinases (RTKs), which subsequently activate intracellular signaling intermediates and regulate translational [67]. Importantly, MAPK signaling pathways are also critical mediators of inflammatory responses [68]. In the present study, PS-MPs exposure up-regulated multiple MAPK-associate genes, including MAPK8IP3, FGFR1, HSPB1, TAOK2, RRAS2, PAK2, MEF2C, CSF1, NGF, MAPK11, CACNA1C, HSPA1L, TGFB3, and RPS6KA5, which are known to participate in oxidative stress responses, inflammation, tumorigeneses, and cell proliferation.

Inflammation represents highly conserved protective response developed by higher organisms to combat infection and tissue injury. Upon exposure to pathogens or cellular damage, the innate immune system rapidly initiates an inflammatory response that constitutes the first line of host defense. This response activates numerous genes involved in antimicrobial activity and the development of adaptive immunity [69]. Increasing evidence suggests that PS-MPs toxicity is closely linked to inflammatory signaling pathways that promote oxidative stress, tissue damages, and systemic dysfunction. For instance, a recent single-cell RNA sequencing study demonstrated that combined exposure to a high-fat diet and PS-MPs (5 μm, 10 mg/kg) generated pro-inflammatory renal microenvironment characterized by Th17 cells and M1 macrophage infiltration. Elevated levels of IL-17A+ CD4+ T cells, and increased expression IL-17 target genes, including (e.g., S100A8, LCN2) [70]. Additionally, exposure to PS-MP ranging from 50 nm–4 μm has been shown interstitial fibrosis, tubular dilatation, and glomerular atrophy in mice. Immunohistochemistry analysis further demonstrated increased IL-17C expression in injured tubules, while IL-17RA-deficient mice exhibited significantly reduced renal damage [71]. Consequent with these findings, our transcriptomic data showed significant up-regulation of inflammatory genes including IL-17, SCYL3, CCRL2, MYD88, TLR12, ELF3, TNFRS1B, CXCL9, TNFAIP3, and TLR1 in PS-MP-exposed kidneys. These genes are critically involved I inflammatory signaling and immune activation. Collectively, our findings suggest that PS-MPs exposure disrupts renal homeostasis by modulating key signaling pathways including PPARG, IL-17, and MAPK, which are closely associated with oxidative stress and inflammatory responses.

Although this study provides comprehensive evidence supporting PS-MPs-induced nephrotoxicity, several limitations should be acknowledged. The present investigation was conducted exclusively in male mice. Because sex represents an important biological variable that can influence toxicological responses, future studies including female animals are necessary to determine susceptibility to PS-MPs-induced kidney damage is sex-dependent. Furthermore, although phosphate-buffered saline served as an appropriate control vehicle, the absence of key PS-MPs-associated molecular signature, such as activation of PPAR and IL-17 signaling pathways, in control animals supports the conclusion that the observed nephrotoxicity was attributable to PS-MP exposure.

Conclusion

In conclusion, our study demonstrates that mice exposure to polystyrene microplastics at 1mg/kg/day of PS-MPs for 28 days induces significant kidney injury in mice, characterized by structural abnormalities and deregulation of key molecular pathways. These findings indicate that PS-MPs exposure promotes oxidative stress and inflammatory responses in renal tissue, as evidenced by the activation of genes associated with the PPAR signaling pathway, MAPK signaling pathway, and inflammatory responses. Notably, several key mediators involved in these pathogenic mechanisms, including PPAR, IL-17, and MAPK8IP3, were significantly affected. Collectively, these results provide important mechanistic insights into the molecular pathways underlying PS-MP-induced renal toxicity and highlight the potential role of microplastics in contributing to kidney dysfunction.

Declaration

All experimental procedures of this study were approved by the Local Animal Care and Ethics Committee of Yangzhou University (Permit Number: SYXK (SU) IACUC 2012-0033).

Author contributions

A.A.B and A.Y.A and D.C designed research; A.A.B., S.Y.A., C.L., A.A.A., H.-Y.L., W.A.A., H. S., and K.J.O.: conducted research; D.C.: provided essential materials; A.A.B., S.Y.A., and D.C.: analyzed data; A.A.B.: wrote paper D.C.: had primary responsibility for final content; the manuscript draft was critically reviewed and edited by all authors. All authors have read and approved the final manuscript.

Data Availability

The analyzed datasets from this study are available from the corresponding author upon reasonable request. The original RNA sequencing reads have been deposited in the National Center for Biotechnology Information (NCBI) Sequence Read Archive under BioProject accession PRJNA1404607

Funding

This work was funded by the National Key R&D Program of China (2023YFD1301200, 2023YFD1801100), Jiangsu Provincial Double-Innovation Team Program (JSSCTD202147), the Priority Academic Program Development of Jiangsu Higher Education Institutions (PAPD).

References

1. Rodrigues MO, Abrantes N, Gonçalves FJM, Nogueira H, Marques JC, Gonçalves AMM: Impacts of plastic products used in daily life on the environment and human health: What is known? *Environmental Toxicology and Pharmacology* 2019, 72:103239.
2. Jin Y, Lu L, Tu W, Luo T, Fu Z: Impacts of polystyrene microplastic on the gut barrier, microbiota and metabolism of mice. *Sci Total Environ* 2019, 649:308-317.
3. Horton AA, Dixon SJ: Microplastics: An introduction to environmental transport processes. *WIREs Water* 2018, 5:e1268.
4. Wang C, Zhao J, Xing B: Environmental source, fate, and toxicity of microplastics. *Journal of Hazardous Materials* 2021, 407:124357.
5. Andrady AL, Barnes PW, Bornman JF, Gouin T, Madronich S, White CC, Zepp RG, Jansen MAK: Oxidation and fragmentation of plastics in a changing environment; from UV-radiation to biological degradation. *Science of The Total Environment* 2022, 851:158022.
6. Zhang K, Hamidian AH, Tubić A, Zhang Y, Fang JKH, Wu C, Lam PKS: Understanding plastic degradation and microplastic formation in the environment: A review. *Environmental Pollution* 2021, 274:116554.
7. Du H, Xie Y, Wang J: Microplastic degradation methods and corresponding degradation mechanism: Research status and future perspectives. *Journal of Hazardous Materials* 2021, 418:126377.
8. Xiang Y, Jiang L, Zhou Y, Luo Z, Zhi D, Yang J, Lam SS: Microplastics and environmental pollutants: Key interaction and toxicology in aquatic and soil environments. *Journal of Hazardous Materials* 2022, 422:126843.
9. Chen G, Feng Q, Wang J: Mini-review of microplastics in the atmosphere and their risks to humans. *Science of The Total Environment* 2020, 703:135504.
10. Evangeliou N, Grythe H, Klimont Z, Heyes C, Eckhardt S, Lopez-Aparicio S, Stohl A: Atmospheric transport is a major pathway of microplastics to remote regions. *Nature Communications* 2020, 11:3381.
11. Hahladakis JN, Velis CA, Weber R, Iacovidou E, Purnell P: An overview of chemical additives present in plastics: Migration, release, fate and environmental impact during their use, disposal and recycling. *Journal of Hazardous Materials* 2018, 344:179-199.
12. Schymanski D, Goldbeck C, Humpf HU, Fürst P: Analysis of microplastics in water by micro-Raman spectroscopy: Release of plastic particles from different packaging into mineral water. *Water Res* 2018, 129:154-162.
13. Pivokonsky M, Cermakova L, Novotna K, Peer P, Cajthaml T, Janda V: Occurrence of microplastics in raw and treated drinking water. *Sci Total Environ* 2018, 643:1644-1651.
14. Herzke D, Anker-Nilssen T, Nøst TH, Götsch A, Christensen-Dalsgaard S, Langset M, Fangel K, Koelmans AA: Negligible Impact of Ingested Microplastics on Tissue Concentrations of Persistent Organic Pollutants in Northern Fulmars off Coastal Norway. *Environ Sci Technol* 2016, 50:1924-1933.
15. Abbasi S, Soltani N, Keshavarzi B, Moore F, Turner A, Hassanaghaei M: Microplastics in different tissues of fish and prawn from the Musa Estuary, Persian Gulf. *Chemosphere* 2018, 205:80-87.
16. Cho Y, Shim WJ, Jang M, Han GM, Hong SH: Abundance and characteristics of microplastics in market bivalves from South Korea. *Environ Pollut* 2019, 245:1107-1116.
17. Li J, Green C, Reynolds A, Shi H, Rotchell JM: Microplastics in mussels sampled from coastal waters and supermarkets in the United Kingdom. *Environmental Pollution* 2018, 241:35-44.
18. Li Y, Chen L, Zhou N, Chen Y, Ling Z, Xiang P: Microplastics in the human body: A comprehensive review of exposure, distribution, migration mechanisms, and toxicity. *Science of The Total Environment* 2024, 946:174215.
19. Carbery M, O'Connor W, Palanisami T: Trophic transfer of microplastics and mixed contaminants in the marine food web and implications for human health. *Environment International* 2018, 115:400-409.
20. Yang YF, Chen CY, Lu TH, Liao CM: Toxicity-based toxicokinetic/toxicodynamic assessment for bioaccumulation of polystyrene microplastics in mice. *J Hazard Mater* 2019, 366:703-713.
21. Bocker R, Silva EK: Microplastics in our diet: A growing concern for human health. *Science of The Total Environment* 2025, 968:178882.
22. Fayshal MA: Current practices of plastic waste management, environmental impacts, and potential alternatives for reducing pollution and improving management. *Heliyon* 2024, 10:e40838.

23. Zeng L, Li L, Xiao J, Zhou P, Han X, Shen B, Dai L: Microplastics in the Environment: A Review Linking Pathways to Sustainable Separation Techniques. In *Separations*, vol. 122025.
24. Li Z, Xu T, Peng L, Tang X, Chi Q, Li M, Li S: Polystyrene nanoplastics aggravates lipopolysaccharide-induced apoptosis in mouse kidney cells by regulating IRE1/XBP1 endoplasmic reticulum stress pathway via oxidative stress. *Journal of Cellular Physiology* 2023, 238:151-164.
25. Wang YL, Lee YH, Hsu YH, Chiu IJ, Huang CC, Huang CC, Chia ZC, Lee CP, Lin YF, Chiu HW: The Kidney-Related Effects of Polystyrene Microplastics on Human Kidney Proximal Tubular Epithelial Cells HK-2 and Male C57BL/6 Mice. *Environ Health Perspect* 2021, 129:57003.
26. Yu P, Liu Z, Wu D, Chen M, Lv W, Zhao Y: Accumulation of polystyrene microplastics in juvenile Eriocheir sinensis and oxidative stress effects in the liver. *Aquatic Toxicology* 2018, 200:28-36.
27. Prata JC, da Costa JP, Duarte AC, Rocha-Santos T: Suspected microplastics in Atlantic horse mackerel fish (Trachurus trachurus) captured in Portugal. *Marine Pollution Bulletin* 2022, 174:113249.
28. Sui M, Lu Y, Wang Q, Hu L, Huang X, Liu X: Distribution patterns of microplastics in various tissues of the Zhikong scallop (Chlamys farreri) and in the surrounding culture seawater. *Marine Pollution Bulletin* 2020, 160:111595.
29. Tang Y, Zhao R, Pu Q, Jiang S, Yu F, Yang Z, Han T: Investigation of nephrotoxicity on mice exposed to polystyrene nanoplastics and the potential amelioration effects of DHA-enriched phosphatidylserine. *Science of The Total Environment* 2023, 892:164808.
30. Meng X, Yin K, Zhang Y, Wang D, Lu H, Hou L, Zhao H, Xing M: Polystyrene microplastics induced oxidative stress, inflammation and necroptosis via NF-κB and RIP1/RIP3/MLKL pathway in chicken kidney. *Toxicology* 2022, 478:153296.
31. Derosa G, Sahebkar A, Maffioli P: The role of various peroxisome proliferator-activated receptors and their ligands in clinical practice. *Journal of Cellular Physiology* 2018, 233:153-161.
32. Masenga SK, Desta S, Hatcher M, Kirabo A, Lee DL: How PPAR-alpha mediated inflammation may affect the pathophysiology of chronic kidney disease. *Current Research in Physiology* 2025, 8:100133.
33. Corrales P, Izquierdo-Lahuerta A, Medina-Gómez G: Maintenance of Kidney Metabolic Homeostasis by PPAR Gamma. *Int J Mol Sci* 2018, 19.
34. Cuarental L, Sucunza-Sáenz D, Valiño-Rivas L, Fernandez-Fernandez B, Sanz AB, Ortiz A, Vaquero JJ, Sanchez-Niño MD: MAP3K kinases and kidney injury. *Nefrología (English Edition)* 2019, 39:568-580.
35. Matsuzawa A, Ichijo H: Redox control of cell fate by MAP kinase: physiological roles of ASK1-MAP kinase pathway in stress signaling. *Biochimica et Biophysica Acta (BBA) - General Subjects* 2008, 1780:1325-1336.
36. Deng Y, Zhang Y, Lemos B, Ren H: Tissue accumulation of microplastics in mice and biomarker responses suggest widespread health risks of exposure. *Sci Rep* 2017, 7:46687.
37. Bocker R, Silva EK: Microplastics in our diet: A growing concern for human health. *Sci Total Environ* 2025, 968:178882.
38. Severgnini M, Sherman J, Sehgal A, Jayaprakash NK, Aubin J, Wang G, Zhang L, Peng CG, Yucius K, Butler J, Fitzgerald K: A rapid two-step method for isolation of functional primary mouse hepatocytes: cell characterization and asialoglycoprotein receptor based assay development. *Cytotechnology* 2012, 64:187-195.
39. Subramanian A, Tamayo P, Mootha VK, Mukherjee S, Ebert BL, Gillette MA, Paulovich A, Pomeroy SL, Golub TR, Lander ES, Mesirov JP: Gene set enrichment analysis: a knowledge-based approach for interpreting genome-wide expression profiles. *Proc Natl Acad Sci U S A* 2005, 102:15545-15550.
40. Wu B, Xi S: Bioinformatics analysis of differentially expressed genes and pathways in the development of cervical cancer. *BMC Cancer* 2021, 21:733.
41. Zhou Y, Zhou B, Pache L, Chang M, Khodabakhshi AH, Tanaseichuk O, Benner C, Chanda SK: Metascape provides a biologist-oriented resource for the analysis of systems-level datasets. *Nat Commun* 2019, 10:1523.
42. Goodman KE, Hua T, Sang Q-XA: Effects of Polystyrene Microplastics on Human Kidney and Liver Cell Morphology, Cellular Proliferation, and Metabolism. *ACS Omega* 2022, 7:34136-34153.
43. Carbery M, O'Connor W, Palanisami T: Trophic transfer of microplastics and mixed contaminants in the marine food web and implications for human health. *Environ Int* 2018, 115:400-409.
44. Wardoyo AYP, Juswono UP, Noor JAE: Varied dose exposures to ultrafine particles in the motorcycle smoke cause kidney cell damages in male mice. *Toxicol Rep* 2018, 5:383-389.
45. Zou H, Chen Y, Qu H, Sun J, Wang T, Ma Y, Yuan Y, Bian J, Liu Z: Microplastics Exacerbate Cadmium-Induced Kidney Injury by Enhancing Oxidative Stress, Autophagy, Apoptosis, and Fibrosis. In *International Journal of Molecular Sciences*, vol. 232022.
46. Meng X, Zhang J, Wang W, Gonzalez-Gil G, Vrouwenvelder JS, Li Z: Effects of nano- and microplastics on kidney: Physicochemical properties, bioaccumulation, oxidative stress and immunoreaction. *Chemosphere* 2022, 288:132631.
47. Wang W, Guan J, Feng Y, Nie L, Xu Y, Xu H, Fu F: Polystyrene microplastics induced nephrotoxicity associated with oxidative stress, inflammation, and endoplasmic reticulum stress in juvenile rats. *Front Nutr* 2022, 9:1059660.
48. Deng Y, Zhang Y, Lemos B, Ren H: Tissue accumulation of microplastics in mice and biomarker responses suggest widespread health risks of exposure. *Scientific Reports* 2017, 7:46687.
49. Karmakova T, Sergeeva NS, Kanukoev K Y, Alekseev BY, Kaprin A D: Kidney Injury Molecule 1 (KIM-1): a Multifunctional Glycoprotein and Biological Marker (Review). *Sovrem Tekhnologii Med* 2021, 13:64-78.
50. Brilland B, Boud'hors C, Wacrenier S, Blanchard S, Cayon J, Blanchet O, Piccoli GB, Henry N, Djema A, Coindre J-P, et al: Kidney injury molecule 1 (KIM-1): a potential biomarker of acute kidney injury and tubulointerstitial injury in patients with ANCA-glomerulonephritis. *Clinical Kidney Journal* 2023, 16:1521-1533.

51. Sheng S, Han N, Wei Y, Wang J, Han W, Xing B, Xing M, Zhang W: Liver Injury Induced by Exposure to Polystyrene Microplastics Alone or in Combination with Cadmium in Mice Is Mediated by Oxidative Stress and Apoptosis. *Biological Trace Element Research* 2023, 202:2170-2183.
52. 刘玲玲: Role of HO-1 in sevoflurane-induced improvement in sepsis-associated encephalopathy in mice. *Chinese Journal of Anesthesiology* 2021.
53. Yuan Z, Li J, Xiao F, Wu Y, Zhang Z, Shi J, Qian J, Wu X, Yan F: Sinensetin protects against periodontitis through binding to Bach1 enhancing its ubiquitination degradation and improving oxidative stress. *International Journal of Oral Science* 2024, 16.
54. Shahidi Dadras M, Rakhshan A, Dadkhahfar S, Barat T: The role of interleukin‐17 (IL‐17) in the pathogenesis of discoid lupus erythematosus and lichen planopilaris: is immunohistochemistry for IL‐17 a promising way to differentiate these entities? *International Journal of Dermatology* 2021, 61:647-652.
55. Feng L, Chen C, Xiong X, Wang X, Li X, Kuang Q, Wei X, Gao L, Niu X, Li Q, et al: PS-MPs promotes the progression of inflammation and fibrosis in diabetic nephropathy through NLRP3/Caspase-1 and TGF-β1/Smad2/3 signaling pathways. *Ecotoxicology and Environmental Safety* 2024, 273:116102.
56. Zheng J, Tan Z, Wu J, Liu J, Yang T, Yang H: Polystyrene microplastics aggravate acute pancreatitis in mice. *Toxicology* 2023, 491:153513.
57. Li R, Zhu L, Cui L, Zhu Y-G: Viral diversity and potential environmental risk in microplastic at watershed scale: Evidence from metagenomic analysis of plastisphere. *Environment International* 2022, 161:107146.
58. Fulda S, Gorman AM, Hori O, Samali A: Cellular stress responses: cell survival and cell death. *Int J Cell Biol* 2010, 2010:214074.
59. Jabbari P, Mona S, and Rezaei N: An inflammatory triangle in Sarcoidosis: PPAR-γ, immune microenvironment, and inflammation. *Expert Opinion on Biological Therapy* 2021, 21:1451-1459.
60. Chen H, Tan H, Wan J, Zeng Y, Wang J, Wang H, Lu X: PPAR-γ signaling in nonalcoholic fatty liver disease: Pathogenesis and therapeutic targets. *Pharmacology & Therapeutics* 2023, 245:108391.
61. Adam SY, Muniyappan M, Huang H, Ennab W, Liu HY, Ahmed AA, Sun MA, Dessie T, Kim IH, Hu Y, et al: Dietary Organic Zinc Supplementation Modifies the Oxidative Genes via RORγ and Epigenetic Regulations in the Ileum of Broiler Chickens Exposed to High-Temperature Stress. *Antioxidants (Basel)* 2024, 13.
62. Liu H-Y, Gu H, Li Y, Hu P, Yang Y, Li K, Li H, Zhang K, Zhou B, Wu H, et al: Dietary Conjugated Linoleic Acid Modulates the Hepatic Circadian Clock Program via PPARα/REV-ERBα-Mediated Chromatin Modification in Mice. 2021, Volume 8 - 2021.
63. Berger JP, Akiyama TE, Meinke PT: PPARs: therapeutic targets for metabolic disease. *Trends Pharmacol Sci* 2005, 26:244-251.
64. Cheng CF, Chen HH, Lin H: Role of PPARα and Its Agonist in Renal Diseases. *PPAR Res* 2010, 2010:345098.
65. Plotnikov A, Flores K, Maik-Rachline G, Zehorai E, Kapri-Pardes E, Berti DA, Hanoch T, Besser MJ, Seger R: The nuclear translocation of ERK1/2 as an anticancer target. *Nat Commun* 2015, 6:6685.
66. Chapnick DA, Warner L, Bernet J, Rao T, Liu X: Partners in crime: the TGFβ and MAPK pathways in cancer progression. *Cell Biosci* 2011, 1:42.
67. Cargnello M, Roux PP: Activation and function of the MAPKs and their substrates, the MAPK-activated protein kinases. *Microbiol Mol Biol Rev* 2011, 75:50-83.
68. Schett G, Elewaut D, McInnes IB, Dayer JM, Neurath MF: How cytokine networks fuel inflammation: Toward a cytokine-based disease taxonomy. *Nat Med* 2013, 19:822-824.
69. Ahmed AU, Williams BR, Hannigan GE: Transcriptional Activation of Inflammatory Genes: Mechanistic Insight into Selectivity and Diversity. *Biomolecules* 2015, 5:3087-3111.
70. Wenhao X, Shiqi Y, Wangrui L, Huaqi G, Linhui Z, Shiyin W, Aihetaimujiang A, Kun C, Guilherme M, Hailiang Z, et al: Single-cell RNA-seq analysis decodes the kidney microenvironment induced by polystyrene microplastics in mice receiving a high-fat diet. *Journal of Nanobiotechnology* 2024, 22.
71. Yung-Li W, Yu-Hsuan L, Yung-Ho H, Chiu IJ, Cathy Chia-Yu H, Chih-Chia H, Zi-Chun C, Chung-Pei L, Yuh-Feng L, Hui-Wen C: The Kidney-Related Effects of Polystyrene Microplastics on Human Kidney Proximal Tubular Epithelial Cells HK-2 and Male C57BL/6 Mice. *Environmental Health Perspectives* 2021, 129.